Preparation of organic-phased TiO_2 nanotube array electrode with higher quantum efficiency and its catalytic degradation on Methylene blue

Nannan Zhen, Yubin Tang*, Wei Teng*

College of Chemistry and Environmental Engineering, Jiangsu University of Science and Technology, Jiangsu 212000, China.

Email: ybbill@163.com, tengw@just.edu.cn

Keywords: TiO_2 nanotube array electrode; anodizing; catalytic; Methylene blue

Abstract. A series of organic-phased TiO_2 nanotube array electrodes were synthesized with different water content, voltage and time by anodic oxidation of Ti foil in $C_2H_6O_2/NH_4F/H_2O$ electrolyte. The structure and optical properties of the TiO_2 nanotube array electrodes were characterized by scanning electron microscopy (SEM), X-ray diffraction (XRD) and Photoelectrochemical techniques. The results show that the TiO_2 nanotube array electrode, which was prepared by 2vol% H_2O electrolyte and 60V direct current(DC) voltage with an increasing rate of $0.1V \cdot s^{-1}$, exhibited a distinguishable orderly array structure and higher quantum efficiency. The as prepared TiO_2 nanotube array electrode presented a positive photoelectrocatalytic effect on removing Methylene blue (MB) from the aqueous solution.

Introduction

Well-ordered arrays of one-dimensional semiconductors have attracted much interest in the last decade as electrode architectures for optoelectronic applications. 1D TiO_2 nanotube arrays (TiO_2-NTs) prepared by the electrochemical anodization on Ti foil have been investigated by many researchers in recent years. [1–5] Several recent studies indicated that TiO_2-NTs had improved properties compared to any other form of titania for photocatalysis,[6,7] the generation of hydrogen from water splitting,[8,9] solar energy conversion,[10–12] the anodes of lithium ion batteries [3,13] sensors for detecting chemical oxygen demands[14]and trace levels hydrogen gas.[15] However, because of its large band gap (3.05eV for rutile and 3.15eV for anatase),[16] the activation of its photocatalytic capability requires ultraviolet light ($\lambda < 400nm$) that contributes less than 5% of the total energy of the solar spectrum.[6,17,18] In addition, the low efficiency of electron–hole separation limits the practical application of TiO_2-NTs in photoelectrochemical and photocatalytic processes.[19–21] To overcome these problems, many modified approaches have been reported.[22–24]

In this study, we have performed a thorough experimental study to determine the ideal parameters for the TiO_2 nanotube array electrode. A series of organic-phased TiO_2 nanotube array electrodes were

successfully synthesized with different water content, voltage and time by the anodic oxidation on Ti foil in $C_2H_6O_2/NH_4F/H_2O$ electrolyte. The structure and optical properties of the TiO_2 nanotube array electrodes were also characterized by SEM, XRD and electrochemical techniques. The photocatalytic activity of the TiO_2 nanotube array electrode was evaluated by degrading MB in aqueous solution.

Experimental

Preparation of the TiO_2-NTs.

Titanium foil (0.5 mm thick, 99.7% purity) was obtained from Beijing Academy of Steel Service, China. All the other chemicals were of analytical grade and were used as received without further purification. Prior to anodization, the Ti foil (2×4 cm^2) was first mechanically polished with different abrasive papers, and then rinsed in an ultrasonic bath of ethanol for 10 min and deionized water for 10 min in turn. The pretreated Ti foils were chemically etched by immersing in a mixture of HF and HNO_3 ($HF/HNO_3/H_2O$ = 1:4:5 in volume) for 30 s, and finally rinsed in deionized water.

The electrochemical anodization was carried out in a two-electrode electrochemical cell connected to a DC power supply. Ti foil served as anodic electrode and Pt foil as the cathode. Detailed experimental conditions can be found in Table. 1.

Table. 1 Different experimental conditions

Sample	Voltage[V]	Time[h]	Water content[vol %]	rate of pressurization[$V\cdot s^{-1}$]
1	60	1	2	-
2	60	1	2	0.1
3	60	0.5	2	-
4	60	0.5	2	0.1
5	60	1.5	2	-
6	60	1.5	2	0.1
7	60	1	5	-
8	60	1	5	0.1
9	60	0.5	5	-
10	60	0.5	5	0.1
11	60	1.5	5	-
12	60	1.5	5	0.1
13	60	1	10	-
14	60	1	10	0.1
15	60	0.5	10	-
16	60	0.5	10	0.1
17	60	1.5	10	-
18	60	1.5	10	0.1

After anodic oxidation, the samples were annealed at 723.15 K in oxygen for 2 h with heating and cooling rates of 2 ˚C·min $^{-1}$ to convert the amorphous phase to the crystalline one.

Characterization.

The morphology of the TiO_2-NTs was characterized using SEM(JSM-5600LV) with an accelerating voltage of 30.02 kV.

XRD was performed on a Rigaku model D/Max-γB diffractometer with Cu K_α radiation.

The electro-chemical measurements were controlled by using a CHI 660E electrochemical workstation. It was carried out in a conventional three-electrode cell containing the TiO_2-NTs anode, a Pt foil counter electrode and a SCE as the reference electrode.

The Photoelectrocatalytic (PEC) oxidation of MB was carried out in a round-bottom quartz reactor. All of the experiments were performed with magnetic stirring, using 0.01 M Na_2SO_4 as the electrolyte. A 500-W high-pressure xenon short arc lamp (Beijing Au Light, China) was used as the visible-light source to provide a light intensity of 12.6 mW cm^{-2}. The initial concentration of the Methylene blue aqueous solution was 20 mg/L. Dark (adsorption) experiments were carried out for 30 min, under continuous stirring, to allow sufficient MB to be adsorbed onto the surface of the catalyst.

Results and Discussion

Structural characterization of material.

The SEM image in Fig. 1 show the top view of a typical array of well-ordered TiO_2-NTs prepared under different way of applied voltage. The average diameter of these nanotubes is found to be 200 nm. Fig. 1(a) and (b) TiO_2-NTs were given a directly voltage to 60V. The anodizing voltage of the sample in Fig 1(c) and (d) was varied from 0 to 60 V with an increasing rate of 0.1 V·s^{-1}.

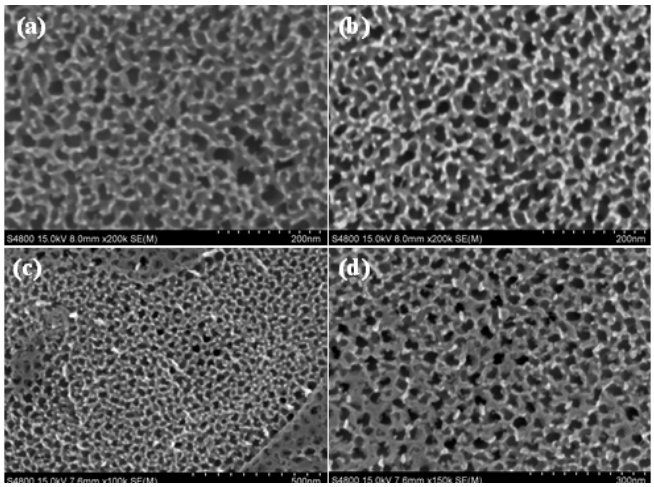

Fig. 1 SEM image of TiO_2 nanotube array electrode prepared under different voltage.(a) and (b) TiO_2-NTs were given a directly voltage to 60v.(c) and (d) the anodizing voltage varied from 0 to 60 V with an increasing rate of 0.1 V·s^{-1}.

Fig. 2 shows the SEM image of the TiO_2-NTs, which had different water content in the electrolyte during the anodic oxidation process. Fig. 2(a) and (b) suggests that the TiO_2-NTs has a better orderly tubular structure with 2vol% H_2O. With the increase of water content in the electrolyte, surface of the TiO_2-NTs has changed. As shown in Fig. 2(c) and (d), when it increased to 5vol% H_2O, a sharply induce of tubular structure appeared on the surface, which was replaced by many pores. As it was continued to increase to 10vol% H_2O, tubular structure on the surface of the electrode decreased gradually, which can be seen in Fig. 2(e) and (f).

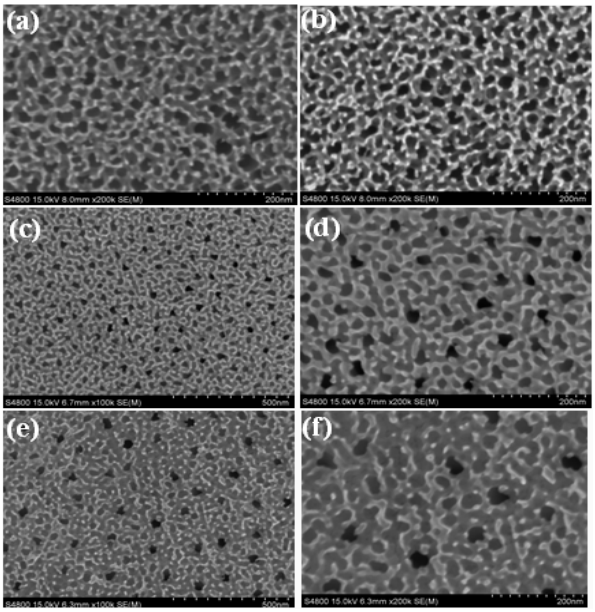

Fig. 2 SEM of TiO_2 nanotube array electrodes with different water content in the electrolyte. (a) and (b) water content was 2vol%. (c) and (d) water content was 5vol%. (e) and (f)water content was 10vol%.

To investigate the influence of the time of anodic oxidation, the results are shown in Fig. 3. It can be seen from the diagram (a) and (b). The TiO_2-NTs exhibited straight tube array structure and the entire electrode surface evenly when the anode oxidation time is 0.5 h. As the extension of the time, some TiO_2 nanotubes disappeared, but formed some holes as shown in (c) and (d). When the anodic oxidation time was extended to 1.5 h, as shown in (e) and (f), the size of the formed pores decreased. The irregular pore structure will be inconducive to the electrode for electron transfer in the process of photoelectrocatalysis, at the same time it also greatly reduces the specific surface area of the TiO_2 nanotube electrode, which will be harmful to the electrode activity in photoelectrocatalysis.

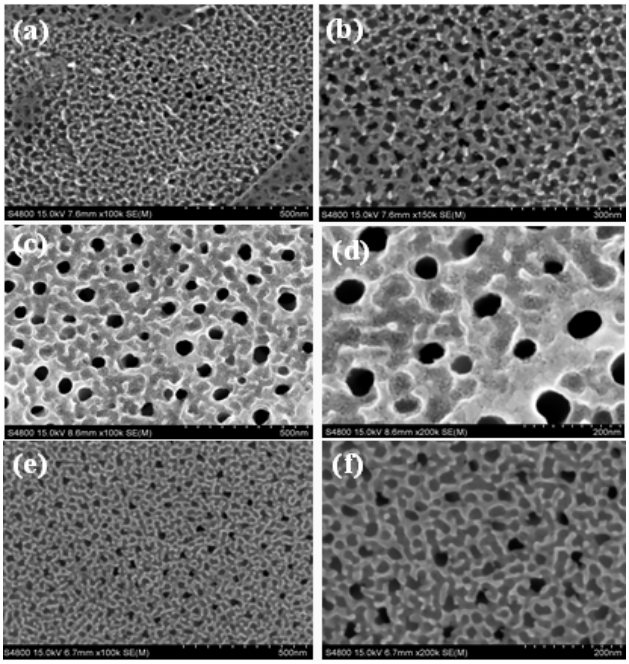

Fig. 3 SEM image of TiO_2-NTs prepared at different times. (a) and (b) anodic oxidation time was 0.5h. (c) and (d) anodic oxidation time was 1h. (e) and (f) anodic oxidation time was 1.5h.

In addition, the structure of the organic-phased TiO_2-NTs and inorganic-phased TiO_2-NTs are characterized by XRD. As shown in Fig. 4, all the diffraction peaks can be well-indexed by the anatase phase of TiO_2 (JCPDS No. 211272) and Ti metal phase (JCPDS No. 050682). Clearly, the organic-phased TiO_2-NTs has crystallized structure with diffraction of anatase (2θ=25.6°), which shows higher catalytic activity in the photocatalytic process. The results of XRD patterns indicate that the organic-phased TiO_2-NTs have better crystal structure than inorganic-phased TiO_2-NTs.

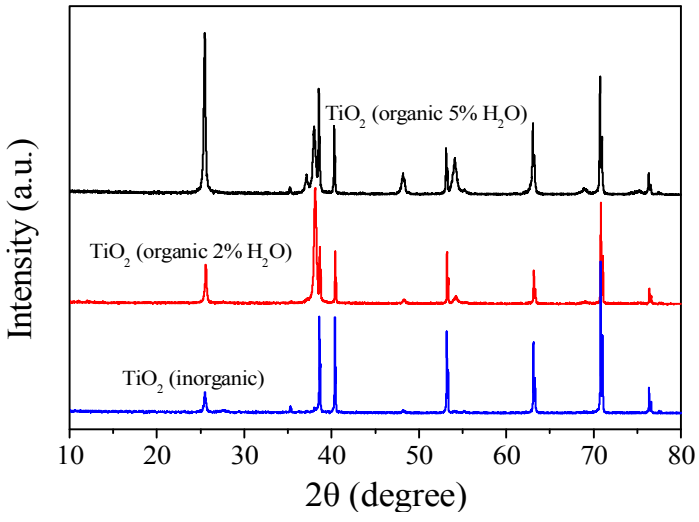

Fig. 4 XRD patterns of the organic-phased TiO_2-NTs and inorganic-phased TiO_2-NTs

Photoelectrochemical measurements.

Representative current density versus voltage (I-V) characteristics of the as-prepared electrodes are presented in Fig. 5. As shown in Fig. 5a, a significant increase in the photocurrent density was observed for the TiO_2-NTs under simulated sunlight irradiation for sample 2. Whereas the sample1 exhibited a lower photocurrent density due to the voltage increases rapidly, resulting in the uniform structure on the bottom of the TiO_2-NTs, which affected the photoproduction electronic transfer under light conditions. Under simulated sunlight irradiation, the TiO_2-NTs of sample 4 has the highest photocurrent density(Fig. 5b), which is consistent with the results of the SEM. Fig. 5c shows the changes in the photocurrent density with the ditterent anodic oxidation time. The results show that the shorter of the anodic oxidation time, the higher of the photocurrent response, it also corresponds well to the sample 10 and sample 16. This is mainly because of the extension of the anodic oxidation reaction time, the length of the nanotubes are increased. When the reaction time is 1.5 h, due to the length of the TiO_2 nanotubes is too long, resulting in the increasing of the path for the electron transfer between Ti substrate and TiO_2 nanotubes. This is not conducive to the improvement of the performance during the photoelectroccatalysis process. Moreover, Fig.5d shows that the organic-phased TiO_2 nanotube array electrodes exhibited a distinguishable higher quantum efficiency .

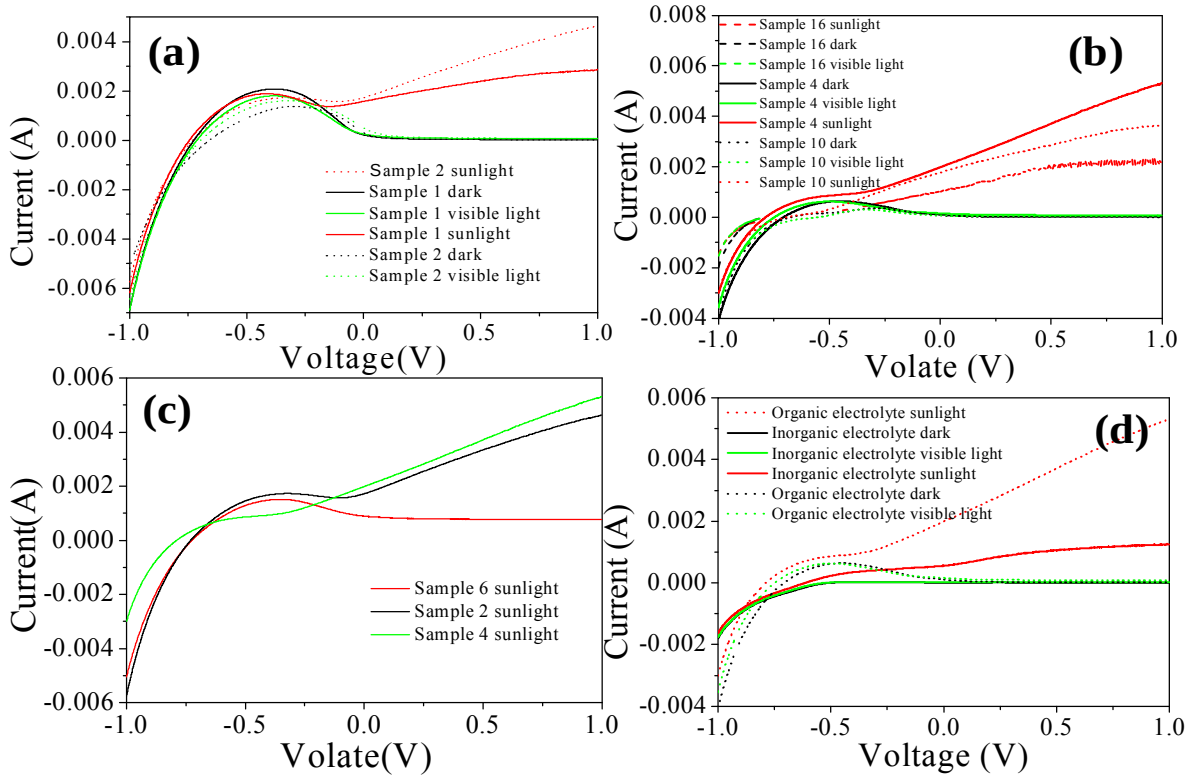

Fig.5 I-V curves of TiO_2 nanotube arrays prepared by different experimental factors under different illumination conditions

Photocatalytic activity.

The performance of different materials in the photoelectrocatalysis process is shown in Fig. 6. The diagram show that the TiO_2 nanotube array electrode, which was prepared by 2vol% H_2O electrolyte and 60V DC voltage with an increasing rate of $0.1V \cdot s^{-1}$, exhibited a positive catalytic effect on removing MB from the aqueous solution. Under simulated sunlight irradiation, nearly 65% of MB was degraded in the photoelectrocatalytic process after 120 min. However, MB exhibited a very low degradation rate under the same condition by the other TiO_2-NTs, which is consistent with the photoelectrochemical measurement results. On the one hand, this is due to the change of the TiO_2 electrode tube array structure. On the other hand, it can also reduces the electrode specific surface area, which effects the target pollutants adsorbed on the surface of the TiO_2-NTs, as mentioned above, resulting in the photoelectric efficiency of the catalytic degradation of MB is decreased obviously.

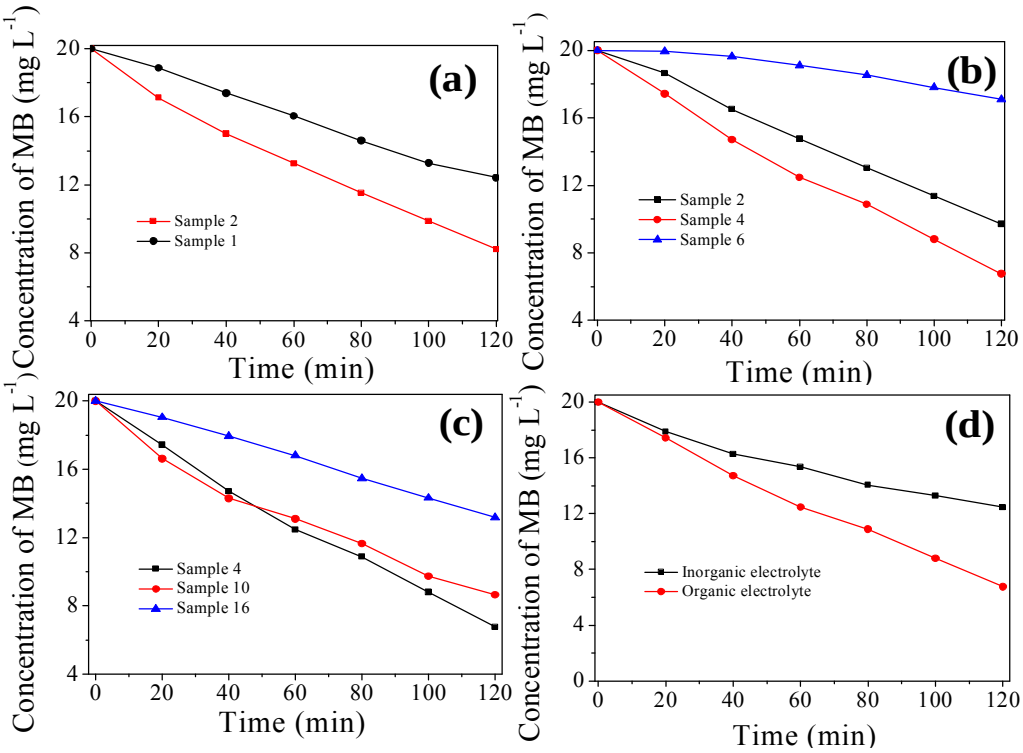

Fig. 6 Decontamination of MB by photoelectrocatalysis with the prepared TiO_2-NTs by different experimental conditions

Conclusion

In Summary, we have performed a thorough experimental study to determine the ideal parameters for the organic-phased TiO_2 nanotube array electrode. The results show that the TiO_2 nanotube array electrode, which was prepared by 2vol% H_2O electrolyte and 60V DC voltage with an increasing rate of $0.1V \cdot s^{-1}$, exhibited a distinguishable orderly array structure and higher quantum efficiency and presented a positive catalytic effect on removing MB from the aqueous solution.

Acknowledgements

This work was supported financially by the National Nature Science Foundation of China (21407067), the Natural Science Foundation of Jiangsu Province (BK20140506).

References

[1] E. Matykina, A. Conde, J. de Damborenea, D. M. y. Marero and M. A. Arenas, Electrochim. Acta, 2011, 56, 9209-9218.

[2] N. K. Allam, K. Shankar and C. A. Grimes, Adv. Mater., 2008, 20, 3942-3946.

[3] J. Idígoras, T. Berger and J. A. Anta, J. Phys. Chem. C, 2013, 117, 1561-1570.

[4] I. Hanzu, T. Djenizian and P. Knauth, J. Phys. Chem. C, 2011, 115, 5989-5996.

[5] G. K. Mor, O. K. Varghese, R. H. T. Wilke, S. Sharma, K. Shankar, T. J. Latempa, K. S. Choi and C. A. Grimes, Nano Lett., 2008, 8, 1906-1911.

[6] X. Chen and S. S. Mao, Chem. Rev., 2007, 107, 2891-2959.

[7] A. El Ruby Mohamed and S. Rohani, Energy Environ. Sci., 2011, 4, 1065-1086.

[8] K. Shankar, J. I. Basham, N. K. Allam, O. K. Varghese, G. K. Mor, X. Feng, M. Paulose, J. A. Seabold, K. S. Choi and C. A. Grimes, J. Phys. Chem. C, 2009, 113, 6327-6359.

[9] R. M. Navarro, M. C. Alvarez Galván, J. A. Villoria de la Mano, S. M. Al-Zahrani and J. L. G. Fierro, Energy Environ. Sci., 2010, 3, 1865-1882.

[10] K. Zhu, N. R. Neale, A. Miedaner and A. J. Frank, Nano Lett., 2007, 7, 69-74.

[11] K. Fan, T. Peng, B. Chai, J. Chen and K. Dai, Electrochim. Acta, 2010, 55, 5239-5244.

[12] A. Lamberti, A. Sacco, S. Bianco, D. Manfredi, F. Cappelluti, S. Hernandez, M. Quaglio and C. F. Pirri, Phys. Chem. Chem. Phys., 2013, 15, 2596-2602.

[13] L. Xue, Z. Wei, R. Li, J. Liu, T. Huang and A. Yu, J. Mater. Chem., 2011, 21, 3216-3220.

[14] Q. Zheng, B. Zhou, J. Bai, L. Li, Z. Jin, J. Zhang, J. Li, Y. Liu, W. Cai and X. Zhu, Adv. Mater., 2008, 20, 1044-1049.

[15] O. K. Varghese, D. Gong, M. Paulose, K. G. Ong and C. A. Grimes, Sens. Actuators, B, 2003, 93, 338-344.

[16] A. Bendavid, P. J. Martin, A. Jamting and H. Takikawa, Thin Solid Films, 1999, 355-356, 6-11.

[17] S. Hoang, S. Guo, N. T. Hahn, A. J. Bard and C. B. Mullins, Nano Lett., 2012, 12, 26-32.

[18] K. Dai, H. Chen, T. Peng, D. Ke and H. Yi, Chemosphere, 2007, 69, 1361-1367.

[19] P. Zhang, C. Shao, Z. Zhang, M. Zhang, J. Mu, Z. Guo, Y. Sun and Y. Liu, J. Mater. Chem., 2011, 21, 17746-17753.

[20] H. Chen, K. Dai, T. Peng, H. Yang and D. Zhao, Mater. Chem. Phys., 2006, 96, 176-181.

[21] H. Chen, M. Shen, R. Chen, K. Dai and T. Peng, Environ. Technol., 2011, 32, 1515-1522.

[22] K. Dai, T. Peng, H. Chen, J. Liu and L. Zan, Environ. Sci. Technol., 2009, 43, 1540-1545.
[23] M. Shen, X. Zhang, K. Dai, H. Chen and T. Peng, CrystEngComm, 2013, 15, 1146-1152.
[24] K. Dai, T. Peng, H. Chen, R. Zhang and Y. Zhang, Environ. Sci. Technol., 2008, 42, 1505-1510.